Received: 5 December 2022 | Revised: 20 March 2023 | Accepted: 28 March 2023

DOI: 10.1111/mec.16949

ORIGINAL ARTICLE

MOLECULAR ECOLOGY WILEY

Distinct life history strategies underpin clear patterns of succession in microparasite communities infecting a wild mammalian host

Caroline K. Glidden[1] | Canan Karakoç[2,3,4] | Chenyang Duan[5] | Yuan Jiang[5] | Brianna Beechler[6] | Abdul Jabbar[7] | Anna E. Jolles[1,6]

[1]Department of Integrative Biology, Oregon State University, Corvallis, Oregon, USA

[2]Department of Biology, Indiana University, Bloomington, Indiana, USA

[3]Department of Environmental Microbiology, Helmholtz Centre for Environmental Research—UFZ, Leipzig, Germany

[4]German Centre for Integrative Biodiversity Research (iDiv) Halle-Jena-Leipzig, Leipzig, Germany

[5]Department of Statistics, Oregon State University, Corvallis, Oregon, USA

[6]College of Veterinary Medicine, Oregon State University, Corvallis, Oregon, USA

[7]Department of Veterinary Biosciences, Melbourne Veterinary School, The University of Melbourne, Victoria, Australia

Correspondence
Caroline K. Glidden, Department of Integrative Biology, Oregon State University, Corvallis, OR, USA.
Email: ckglidden@gmail.com

Present address
Caroline K. Glidden, Department of Biology, Stanford University, Stanford, California, USA

Funding information
Achievement Rewards for College Scientists Foundation; Faculty of Veterinary and Agricultural Sciences, University of Melbourne; UK Biotechnology and Biological Sciences Research Council grant, Grant/Award Number: BB/L011085/1; USA National Science Foundation

Handling Editor: Camille Bonneaud

Abstract

Individual animals in natural populations tend to host diverse parasite species concurrently over their lifetimes. In free-living ecological communities, organismal life histories shape interactions with their environment, which ultimately forms the basis of ecological succession. However, the structure and dynamics of mammalian parasite communities have not been contextualized in terms of primary ecological succession, in part because few datasets track occupancy and abundance of multiple parasites in wild hosts starting at birth. Here, we studied community dynamics of 12 subtypes of protozoan microparasites (*Theileria* spp.) in a herd of African buffalo. We show that *Theileria* communities followed predictable patterns of succession underpinned by four different parasite life history strategies. However, in contrast to many free-living communities, network complexity decreased with host age. Examining parasite communities through the lens of succession may better inform the effect of complex within host eco-evolutionary dynamics on infection outcomes, including parasite co-existence through the lifetime of the host.

KEYWORDS
community ecology, disease biology, DNA barcoding, host parasite interactions, life history evolution, metagenomics

1 | INTRODUCTION

Ecological communities are shaped, at the most fundamental level, by the succession of species as they colonize new habitats and subsequently interact with their environment to persist. As such, in the absence of major stochastic extirpation events, communities may follow temporally predictable patterns according to the events that initiate a new habitat patch and the component species' life histories (Leibold & Chase, 2017; Miller & ter Horst, 2012; Noble & Slatyer, 1977; Pickett et al., 1987).

Classical succession theory states that communities increase in diversity through early successional stages, peak at mid-successional stages, and, if the community reaches equilibrium, slightly decline to a stable plateau at late successional stages (Miller & ter Horst, 2012). Mechanistically, patterns of succession are hypothesized to be driven by habitat patch resource availability and species interaction networks. For example, classical ecological theory suggests that species in early successional stages often have life history strategies conducive to high dispersal rates so they can establish in new habitat patches before being displaced by slower dispersing, superior competitors (Tilman, 1994). Early communities may consist of positive and negative interactions, where pioneer species modify the environment to be more or less hospitable for later-colonizing species (Malkinson et al., 2003). In many free-living communities, the resources governing species interactions decrease as species richness increases (e.g., light for plants) leading to equilibrium communities with a higher proportion of negative interactions than early successional communities (Tilman, 1985). However, perturbations at early stages may prohibit communities from reaching a stable equilibrium state or drive communities towards alternative stable states (Connell, 1978; Kröel-Dulay et al., 2015; Lewontin, 1969). Altogether, mechanisms driving patterns of succession are key to understanding and predicting changes in species assemblages over time.

In parasite communities, early research suggested parasite interactions to be rare and community structure to conform to neutral assembly models (Poulin, 2004). Since then, an abundance of work has pointed towards the importance of order of infection and parasite interaction dynamics on parasite community assembly and infection outcome (Budischak et al., 2016; Devevey et al., 2015; Ezenwa & Jolles, 2015; Halliday et al., 2020; Johnson & Hoverman, 2012; Lello et al., 2004; Rynkiewicz et al., 2019; Telfer et al., 2010).

However, few studies have contextualized the structure and dynamics of parasite communities in terms of ecological succession, especially primary succession, in part because few datasets track occupancy and abundance of multiple parasites in wild hosts starting at birth (but see Budischak et al., 2016; Combrink et al., 2020; Espínola-Novelo et al., 2020; Mordecai et al., 2016 for succession based studies in wild systems). Life history trade-offs, such as the commonly observed negative association between dispersal and competitive ability, may play a role in structuring successional processes in parasite communities as they do in free-living systems. However, parasite communities differ from free-living communities in at least two important ways that may impact successional patterns: First, resource availability, especially in terms of space and nutrients, may increase, rather than decrease, over time because hosts (habitat patches) grow as they mature, perhaps resulting in a reduction in negative interactions in later successional communities (Griffiths et al., 2014; Rynkiewicz et al., 2015). Second, hosts, unlike abiotic habitat patches, can directly respond to and impact colonization and persistence through their immune responses (Rynkiewicz et al., 2015). This is likely to affect successional processes in novel ways. For example, negative intra-specific interactions may increase and inter-specific interactions may decrease with animal age as the adaptive immune system develops (i.e. the immune system more precisely targets the focal pathogen species); as such colonization patterns may emerge from interactions with both co-infecting parasites and the host immune system with the relative impact of each interaction changing through time. Further, infection by immunosuppressive parasites may facilitate the colonization of different parasites and trigger community development through positive interactions as opposed to negative (Ezenwa & Jolles, 2015; Johnson et al., 2015; Selik et al., 1984). Thus, while many aspects of parasite community ecology mirror dynamics observed in free-living communities, differences in host biology may lead to disparate patterns of community assembly and mechanisms of co-existence through time.

Here, we studied microparasite communities (*Theileria* spp.) throughout the lifetime of African buffalo to better understand the development of microparasite communities in a natural system. *Theileria* are tick-borne intracellular protists within the phylum Apicomplexa (Norval et al., 1992). African buffalo are reservoir hosts for three species clades (*T. taurotragi*, *T. mutans*, *T. velifera*), which also infect cattle at the wildlife-livestock interface and cause economically significant morbidity and mortality (Mans et al., 2016). In the buffalo host, all *Theileria* have a life stage in which they infect lymphocytes (a type of white blood cell) and red blood cells (Norval et al., 1992). However, *Theileria* within the *T. taurotragi* species clade (*T. parva*, *T.* sp. (bougasvlei), *T.* sp. (buffalo)) primarily replicate within white blood cells of the mammalian host before transfer to red blood cells for uptake by the tick vector; whereas *Theileria* within the *T. mutans* and *T. velifera* clades primarily replicate within red blood cells of the mammalian host (Norval et al., 1992). Protective immunity against *T. parva* (in the T. taurotragi clade) is largely mediated by CD8+ cytotoxic T cells and CD4+ cells associated with Type 1 T helper cells (Baldwin et al., 1992; McKeever et al., 1994)—both of which are typical immune response to intracellular parasites (Janeway et al., 2001). Overall, while initial infection by *Theileria* initiates a broad, non-specific, intracellular immune response, adaptive immunity against *Theileria* is complex and taxon-specific (Mac Hugh et al., 2009; Morrison, 1996).

Individual African buffalo are commonly infected concurrently by up to 12 closely related subtypes of *Theileria* and infection has been detected in animals at all life stages (e.g., calves, juveniles, adults) (Combrink et al., 2020; Glidden et al., 2020; Henrichs et al., 2016). Many of these microparasite subtypes persist through the host's adulthood, co-existing long-term despite close phylogenetic relatedness of parasite subtypes (Glidden et al., 2020). This raises the

question of how *Theileria* subtypes avoid the effects of competition for shared resources (blood cells) and apparent competition due to cross-immunity among subtypes (Budischak et al., 2018; Raberg et al., 2006) and, more generally, how community succession operates in this parasite community.

In brief, we longitudinally sampled a herd of African buffalo, containing newborn calves to adult animals, to ask: (1) do microparasites display life history variation (i.e., variation in strategies used by the microparasites to replicate and persist within individual buffalo and the population) and patterns of succession congruent with classical succession theory?; (2) is succession in these parasite communities driven by the inter-specific facilitative or competitive mechanisms observed in free-living systems? We hypothesize that *Theileria* communities follow predictable patterns of colonization (e.g., age at first infection) as microparasites interact with each other and the host immune response to infect and replicate within immunologically naïve hosts. We expect that competition and facilitation are strongest in juvenile hosts who have lower blood cell counts and lack adaptive immune responses to the full suite of *Theileria* subtypes and that the dynamics of the interaction network will help to illuminate mechanisms underpinning patterns of *Theileria* assembly and co-existence.

2 | METHODS

2.1 | Data collection

2.1.1 | Study system and sample collection

African buffalo included in this study were located in a 900-hectare enclosure within the Kruger National Park (KNP) a 19,000 km^2 preserve, located in northeastern South Africa (S 24 23′ 52″, E 31 46′ 40″). The enclosure is entirely within the KNP and has numerous other wild animals typical of the ecosystem (e.g., giraffe, zebra, warthogs, small mammals and small predators). However, the enclosure excludes mega-herbivores (rhino, hippo, elephant) and large predators (lion, leopard). Study animals graze and breed naturally and find water in seasonal pans and man-made (permanent) water troughs. In extremely dry conditions, supplemental grass and alfalfa hay was supplied. A total of 66 African buffalo were included in the study. However, the size of the study herd fluctuated through time due to natural births and deaths. At any given time, the herd of African buffalo consisted of around 50 buffalo.

The herd was sampled at 2–3 months intervals from February 2014–December 2015 (number of capture time points = 10). Animal capture and sedation protocols have previously been described by (Couch et al., 2017). The study was conducted under South Africa Department of Agriculture, Forestry and Fisheries Section 20 permits Ref 12/11/1, ACUP project number 4478 and 4861, Onderstepoort Veterinary Research Animal Ethics Committee project number 100261-Y5, and the Kruger National Park Animal Care and Use Committee project number JOLAE1157-12.

For animals born during the study, their birth date was recorded and their age was tracked through the study. For animals born before the start of the study, the precise age of animals estimated to be less than 2 years old was assessed from body length and horn length, the precise age of animals estimated to be between 2 and 5 years old was assessed based on incisor emergence patterns, and the precise age of animals estimated to be greater than 5 years old was assessed from tooth wear of incisor one (Jolles, 2007). Animals ranged from zero months to 19.50 years (234 months) old. Body condition was determined by assigning a score from 1 to 5 based on manually palpating four sites (ribs, hips, spine, and tail base); average score was used in all analyses (Ezenwa et al., 2009).

During each capture, 2 mL of whole blood was collected via jugular venipuncture directly into EDTA-coated vacutainers and stored on ice during transport. One millilitre of whole blood was pipetted into sterile microcentrifuge tubes and stored at −80°C until it was used for DNA extractions while the rest of blood was immediately used to measure red and white blood cell counts using an automated haematology analyser (Vet ABC, Scil Animal Care Company).

Quantifying Theileria *spp. community abundance and subtype relative abundance*.

Identically to Glidden et al., 2020, we used high throughput amplicon sequencing to detect and quantify read counts of *Theileria* subtypes using an 18S rRNA sequence specific to piroplasms (*Theileria* spp. and *Babesia* spp.) (Gubbels et al., 1999). Additionally, we used a genus-specific qPCR to measure the total abundance of all *Theileria* subtypes (i.e., community abundance).

DNA was extracted from 200 μL of EDTA blood using DNeasy Blood and Tissue Kit (Qiagen) following the manufacturer's protocol. DNA extractions were shipped to the University of Melbourne, Australia, and stored at −20°C until further testing. The V4 hypervariable fragment (~500 bp) of the 18S rRNA gene of *Theileria* was targeted for amplicon sequencing. Briefly, PCR amplicons were generated using the RLBF (5′–GAG GTA GTG ACA AGA AAT AAC AAT–A3′) and RLBR (5′–TCT TCG ATC CCC TAA CTT TC–3′) primers (Gubbels et al., 1999) using the AmpliTaq Gold 360 mastermix (Life Technologies) in a thermal cycler (Veriti-384™; Applied Biosystem). The first PCR was run for the initial denaturation for 2 min at 94°C followed by 30 cycles of 30 s at 94°C, 30 s at 57°C, and 1 min at 72°C and a final extension of 8 min at 72°C. PCR amplicons were purified using magnetic beads and visualized on 2% E-Gel Agarose Gel stained with SYBR Safe DNA Gel Stain (Thermo Fisher). The second PCR was performed to index the amplicons using the TaKaRa Taq DNA Polymerase (Clontech), and it was run for 2 min at 94°C, 15 cycles of 30 s at 94°C, 30 s at 57°C, 1 min at 72°C, and a final extension of 1 min at 72°C. The PCR products were then purified using magnetic beads, quantified by fluorometry (QuantiFlour® dsDNA System), and normalized. The equimolar pool of amplicons was cleaned again using magnetic beads to concentrate the pool and then measured using an Agilent High-Sensitivity D1000 Tape System (Agilent Technologies). The pool was diluted to 5 nM, and the molarity was confirmed again using the Tape System and sequenced on an Illumina MiSeq Reagent Kit v3 (600 cycle) using 2 × 300 base

pairs paired-end reads. Positive (*Theileria orientalis*) and negative (no DNA template) controls were also included during each step of the experiment.

Sequence data was cleaned, filtered and clustered using SeekDeep (V 2.5.1), a software that can obtain single base pair resolution from amplicon data (Hathaway et al., 2018). FASTQ files from all samples were processed using a within-sample relative abundance cutoff of 1% and the Illumina MiSeq tag, allowing no mismatches. Within the SeekDeep pipeline, sequences that were marked as likely chimeric were removed. Additionally, we removed any sequences that occurred once within the study as this would imply a unique sequence that occurred in one animal at one time point. Phred quality score of each consensus sequence was assessed in FastQC (V. 0.11.7). As the final PCR amplicon is ~460 bp, sequences were retained in the analysis if bases had an average Phred quality score > 30 (1 error per 1000 bases).

Bayesian inference (BI) and neighbour joining (NJ) analyses were conducted to identify sequences to *Theileria* subtype. First, a nonredundant database of all *Theileria* and *Babesia* subtypes known to infect African buffalo, as well as closely related host species, was curated using the existing literature (Mans et al., 2016) and the NCBI database (GenBank). SeekDeep sequences and reference sequences were imported into Mesquite (V 3.51; Maddison & Maddison, 2008) and aligned using MUSCLE (V 3.8.31; Edgar, 2004). For the BI analysis, the likelihood parameters were based on the Akaike Information Criterion (AIC) test in jModeltest V.2.1.10 (Darriba et al., 2012). The likelihood parameters used were TrN + I + G (Nst = 6; rates = invariable + gamma). A Bayesian tree was constructed using the Monte Carlo Markov Chain analysis in MrBayes (V.3.1.2). Four simultaneous tree-building chains were used to calculate posterior probabilities for 2,000,000 generations, saving every 100th tree. A consensus tree was constructed based on the final 75% of trees produced (burnin = 0.25%).

The NJ analyses were conducted in MEGA 7.0 (Kumar et al., 2016) and the nodes were tested for robustness with 10,000 bootstrap replicates. The data format was set to DNA and gaps were treated as missing data. For the substitution model, the substitution type was nucleotide, the method used was the number of differences, substitutions included were transitions and transversions, and rates among sites were uniform. The tree topology was checked for concordance. *Theileria* clades were considered supported if NJ bootstrapping values were >75% and Bayesian posterior probability values were >0.95. Subtype clades were considered supported if NJ bootstrapping values were >75%.

We additionally used a quantitative PCR analysis, described in detail in Glidden et al., 2020, to measure the % of blood cells infected by the *Theileria* genus as a whole (i.e., community abundance). We calculated community abundance from the qPCR result by following (Pienaar et al., 2011). In brief, volume of whole blood used in the qPCR assay was calculated by multiplying the proportion of DNA extraction used in the assay by volume of whole blood used in the DNA extraction. Subsequently, the number of red blood cells in each reaction was then calculated by multiplying the volume (number of microliters) of whole blood used in each reaction by the number of red blood cells per microliter. As the 18S gene of *Theileria* is believed to have two copies per genome (Hayashida et al., 2012), copy number per sample (calculated from the mean of duplicates) was divided by two to obtain the number of parasites per reaction. Parasites in each qPCR reaction per sample were divided by red blood cells per reaction and multiplied by 100 to obtain % parasitemia (i.e., community abundance).

2.2 | Analytical methods

2.2.1 | Characterizing patterns of succession and identifying signatures of trade-offs between dispersal and relative abundance in the climax community

To describe aggregate measures of community composition we used a relative abundance of high-throughput sequencing read counts to quantify alpha diversity (Shannon Index, Inverse Simpson Index) and beta diversity (distance, in Euclidian space, from the community centroid). *Theileria* diversity within-hosts (alpha diversity) and among hosts (beta-diversity) were calculated using the *vegan* package (Oksanen, 2020) in R (R v. 4.0.2). As stated above, community abundance was measured as the number of blood cells infected with *Theileria*. As the relationship between buffalo age (months) and our aggregate community metrics appeared non-linear, we used general additive mixed models to evaluate the relationship between age (independent variable, smooth variable) and the three measures of community composition (dependent variables, gaussian distribution). In each model, the smoothing basis was a penalized spline (p-spline). Animal ID and capture number were included as random intercepts. Model assumptions were tested using quantile-quantile plots and the distribution of deviance residuals. We tested for temporal autocorrelation by visually inspecting the autocorrelation function and partial autocorrelation function plots. Additionally, we fit each model with an AR(1) and AR(2) error structure and used a log-likelihood test to evaluate if including a serial correlation structure improved model fit. We found that including a serial autocorrelation structure (AR(1)) improved model fit for the beta diversity (likelihood ratio comparing the null and AR(1) model = 6.70, p-value = .01) and parasite abundance model (likelihood ratio comparing the null and AR(1) model = 64.63, p-value <.01). Thus, we used models with the AR(1) error structure for our final beta diversity and parasite abundance models. Additionally, community abundance was left skewed, thus we log-transformed percent of cells infected for the analysis. Generalized additive mixed model analysis was conducted in *mcgv* (Wood, 2017) and model diagnostic plots were generated in *gratia* (Simpson, 2022).

We identified unique parasite life histories by analysing the change in mean relative abundance and prevalence of each *Theileria* species by buffalo age (months). The relationship between relative abundance of each *Theileria* subtype and animal age was non-linear, as such we fit this relationship using a penalized

B-spline regression (Duan & Jiang, 2022). In the penalized B-spline regression, we first used generalized estimating equations (GEE) to model the compositionally and longitudinally dependent high-throughput sequencing read counts that represent the abundance of *Theileria* subtypes. To further estimate and distinguish the longitudinal profiles of the parasite abundances, we reparametrized the GEE by writing its original parameters as smooth functions of the animal age, which are then approximated by a linear combination of B-spline basis functions with unknown parameters. Finally, we computed the estimated values of these unknown parameters by applying penalized B-splines, that is, maximizing the sum of the quasi-likelihood function from GEE and a penalty function on the B-spline coefficients that control the smoothness of the B-spline functions (Duan & Jiang, 2022).

After we obtained the B-spline coefficients and thus the fitted longitudinal curves of the parasite relative abundances, we determined a few point estimates indicative of different life history strategies for each *Theileria* subtype: the age of first infection (defined as the age at which the relative abundance exceeds 0.01 for the first time), the maximum relative abundance, the age at the maximum relative abundance, the relative abundance that becomes stable, and the age when the relative abundance becomes stable (defined as the age followed by the longest time interval whose slope of the fitted curve is less than 0.003). We also applied bootstrap to estimate the 95% confidence intervals for these point estimates, in which we took 1000 random samples with replacement as the bootstrap samples.

Age-prevalence curves were created by binning animals within 6-month age categories and calculating the proportion of animals infected out of the total number of animals sampled for each subtype for each age class.

Standard errors for the prevalence of each subtype for each age class were calculated by Equation 1:

$$SE = \frac{\sqrt{\text{No. animals infected} \times (1 - \text{No. animlas infected})}}{\text{No. animals sampled}} \quad (1)$$

To identify signatures of trade-offs between life history traits, we calculated Pearson's correlation coefficients between life history traits of each subtype (excluding rare subtypes). Specifically, we examined the correlation between age at first infection versus relative abundance at equilibrium, mean age at equilibrium versus relative abundance at equilibrium, and mean age at first infection versus mean age at equilibrium.

2.2.2 | Describing the development of the Theileria spp. interaction network through the lifetime of the animal

Prior to analysing *Theileria* interactions, we centre-log-transformed read counts (Gloor et al., 2017). Further, following (Karakoç et al., 2020) missing data points (2% of data in the adult animal dataset) were linearly interpolated using the 'na.approx' function in *zoo* (Zeilis & Grothendieck, 2019).

We tested for non-linear, deterministic causal interactions between pairs of *Theileria* subtypes using convergent cross mapping (CCM), which detects information transfer from one variable to another using nonparametric state space reconstruction (Clark et al., 2015; Sugihara & May, 1990; Takens, 1981). If information transfer is detected, then we assume a causal association between subtypes (facilitation or competition), with the causal direction indicated by the direction of information flow.

Since stable estimates from CCM typically require a time series of at least 30 sequential observations, we pooled time series across captured animals to fill in the state space manifold (Clark et al., 2015; Hsieh et al., 2008). We observed that subtype trajectories in young animals were quite different than in adult animals; as such, we described differences in significant interactions detected during stages of succession by running separate analyses for juvenile animals (≤3 years old) and adult animals (>3 years old). We selected the 3-year age cutoff as this is the buffalo age, on average, that all subtypes reached their average rank in climax communities (see Results). Importantly for pooling replicates using CCM, the trajectories of subtypes were quite similar, but not identical, for animals within these age classes (Figures S2 and S3).

Embedding dimensions (E, time-lags used for state space reconstruction) were chosen using simplex projection which tests the ability of variables to predict their own dynamics through leave-one-out cross-validation. We chose E as the smallest dimension that is within 1% of the best predictive value across the dimensions tested (Clark et al., 2015; Sugihara et al., 2012; Sugihara & May, 1990; Ye et al., 2015). For each age category, our time series for each buffalo was ≤10-time steps; additionally, the shortest time series for the juveniles was 4 whereas the shortest time series for adult animals was 5. Thus, as the maximum embedding dimension should be the square root of the maximum time series length (Cheng & Tong, 1992) but one less than the shortest time series length (Clark et al., 2015), we choose a maximum E of 3 for juvenile animals and 4 for adult animals. We used mean absolute error (MAE) to test predictive ability. We included 29 animals in our adult animal analysis and 27 animals in our juvenile animal analysis. For the juvenile animals, we used all subtypes with the exception of rare subtypes: *T. mutans*-undefined, *T.velifera*-undefined, and *T.* sp. (buffalo). For the adult animals, we used all subtypes except for rare subtypes and *T. mutans* and *T. mutans* MSD as these were found in less than 1/3 of adult buffalo samples (see Results) (Figure 2).

To detect interactions with time-lagged effects, we applied CCM with varying prediction lags (−1 to 0). Significance of results was determined using nonparametric bootstrapping by sampling from the observations with replacement and recalculating statistics for 10,000 iterations to determine 95% confidence intervals. In cases where CCM identified significant causal interactions, we selected the best time lag as the time lag with the best predictive ability (quantified using MAE) at the largest library length. Next, for significant interactions, we computed a series of Jacobian-like matrices to

determine the direction and strength of species interactions in each time step using S-mapping, which is a locally weighted multivariate linear regression (Deyle et al., 2016). S-mapping predicts dynamics from the reconstructed state based on E interacting predictor variables, which can be either time-lagged observations of the target subtype (intraspecific effects) or observations of other subtypes. Variables for S-mapping were selected based on the number of E of each target variable. If the number of E was larger than the number of variables causing the target variable, predictor variables were complemented with the time-lagged observations of the target variables. The linear approximation is conducted locally in state space, giving greater weight to the target points near the current state, and can be interpreted as localized linear approximations of the community matrix at different times. Nonlinearity parameter (θ) for S-mapping was defined based on univariate predictive ability (Sugihara & May, 1990).

We evaluated model assumptions (interactions are non-linear and deterministic) by plotting Pearson's correlation coefficient and MAE by library size, deeming an interaction acceptable to use for the analysis if predictive ability increased and saturated with library size (Clark et al., 2015). Typically, in empirical dynamical modelling, model performance is evaluated by using the first half of the time series to reconstruct the state space and the second half of the time series to evaluate model prediction ability. For our study, we used relatively short time segments (maximum time steps = 10) with a relatively small number of replicates (~30) so reserved the entirety of the time segments to reconstruct the state space. Thus, to evaluate model performance, we randomly subsampled animals at increasing sample sizes (by 2 animals per subsample) and calculated a series of summary statistics to evaluate model performance. For the adult and juvenile analysis, we observed that the average root-mean-square error of significant interactions decreased to a stable plateau with sample size (Text S1; Figures S4 and S5). Thus, we consider our results robust and useable. We performed empirical dynamical modelling using the R package *rEDM*[66] and *EDMhelper* (Karakoç & Clark, 2022) in R (version 3.6.1). We visualized our networks using *igraph* (Csardi & Nepusz, 2006).

3 | RESULTS

We sampled a herd of 66 African buffalo, ranging from newborn animals (0 month) to 19-year-old animals, every 2–3 months for 2 years. Upon their inclusion in the study, 18 animals were less than 6 months old, 23 animals were subadults between 1 year old and 4 years old, and 24 animals were greater than 4.5 years old (reproductively mature adults). In the analysis, we included 488 samples (with each sample representing one per buffalo per capture), with each buffalo sampled an average of 7.5 (95% confidence interval: 7.19–7.73) times. On average, at a single time point, buffalo were infected with 7.3 *Theileria* subtypes (95% confidence interval: 7.18–7.40). However, as described in detail below, the number of *Theileria* subtypes infecting a buffalo at a given time varied substantially with host age.

Theileria *communities follow predictable patterns of succession, characterized by life history variation among subtypes and a colonization–persistence trade-off.*

We found clear, highly predictable successional patterns in *Theileria* community structure. Host age had a significant, non-linear effect on alpha diversity (effective degrees of freedom (edf) = 8.69, p-value <.01; Figure 1a; Figure S1), beta diversity (edf = 8.70, p-value <.01, Figure 1b), and community abundance (edf = 3.70, p-value <.01; Figure 1c). *Theileria* diversity in individual hosts (i.e., alpha diversity) increased and saturated with buffalo age, reflecting sequential colonization of young buffalo by the various *Theileria* subtypes. However, *Theileria* communities among buffalo resembled each other more and more closely with increasing host age, followed by a slow increase in the oldest animals; that is, beta diversity mostly declined with host age, suggesting succession towards a predictable climax community of *Theileria*s in African buffalo. The fraction of host blood cells infected by *Theileria* microparasites—*Theileria* community abundance—peaked during early succession and declined towards a stable equilibrium of moderate infection levels in adult buffalo.

We similarly found clear and predictable patterns in individual subtype occupancy and abundance, with some evidence of life history trade-offs within the *T. mutans* clade. Individual buffalo typically acquired most subtypes of *Theileria* by the time they were 1 year old (Figure 2; Table 1). After the host was >3 years old, relative abundance of most subtypes reached equilibrium-like, steady relative abundances (Figure 2; Table 1). However, we found substantial variation in subtype life histories, driven by variable subtype dynamics in young buffalo and differential abundances in climax communities (Figure 2).

T. velifera, *T.velifera* B, *T. mutans* and *T. mutans* MSD appear to be early colonizers as they were present in most calves at their first sampling time point. Early infection with these subtypes was quite ubiquitous with >75% of animals 0–18 months old infected with all four subtypes (Figure 2a). However, they differed in their persistence patterns: *T. velifera* and *T.velifera* B infected calves at high relative abundances and then persisted at moderate relative abundances in juvenile and adult animals (Figure 2b). Prevalence across all age groups was 100% for *T. velifera* and >75% for *T. velifera* B (Figure 2a). In contrast, *T. mutans* and *T. mutans* MSD were commonly cleared from the host after initial infection: about half of animals cleared *T. mutans* by the time they were 24–30 months old and the majority of animals cleared *T. mutans* MSD by the time they reached 18–24 months of age (Figure 2). As such, these early-arriving subtypes can be divided into two life history groups: Early-persistent (*T. velifera*, *T.velifera* B) and early-ephemeral (*T. mutans*, *T.mutans* MSD).

T. mutans-like 1, *T. mutans*-like 2 and *T. mutans*-like 3 appear to be late colonizers with an average age of first infection >5 months, and *T.mutans*-like 3 not infecting animals until they were on average 10 months old (Table 1). Starting at 18–24 months of age, 100% (standard error = 0) of animals were infected with these three subtypes, suggesting that animals harboured persistent infections throughout their lifetime (Figure 2a). *T. mutans*-like 3 and *T. mutans*-like 1 had the

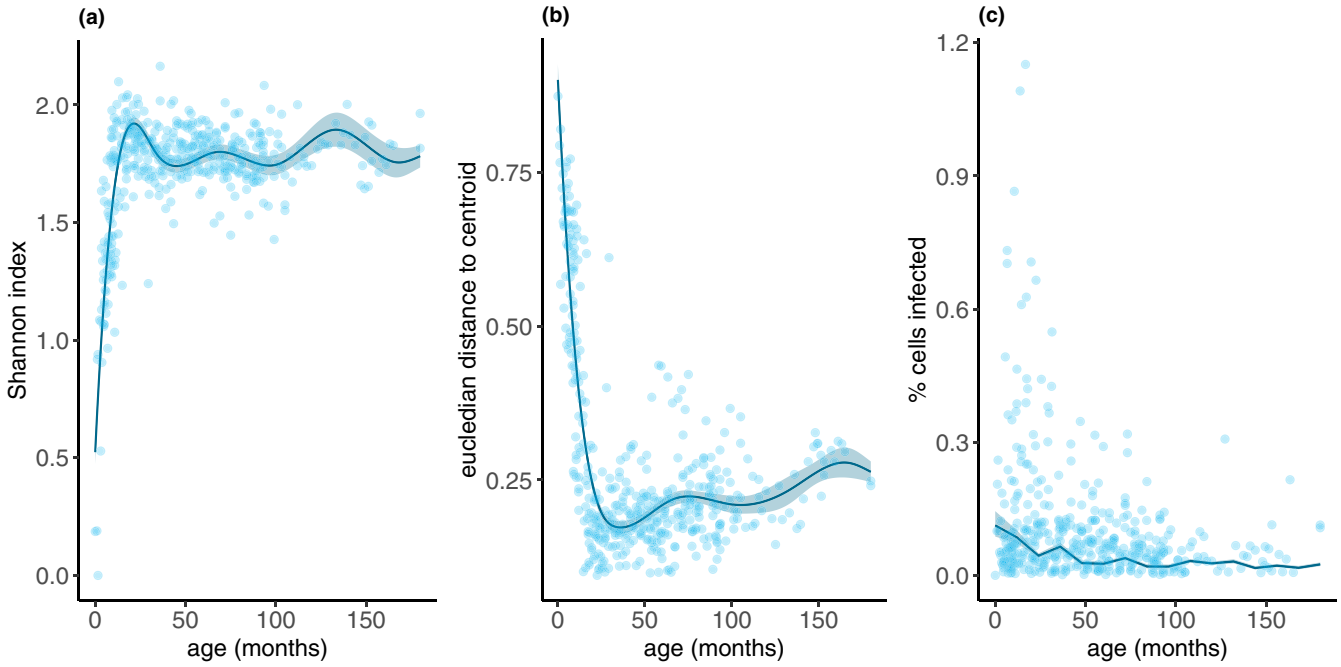

FIGURE 1 Change in aggregate community metrics with age. Points represent observations and lines represent generalized additive mixed model predictions (shaded regions represent standard error). (a) Alpha diversity calculated as Shannon diversity index. (b) Beta diversity calculated as the Euclidean distance to the centroid. (c) Community abundance calculated as per cent of buffalo blood cells infected by all *Theileria* subtypes (% parasitemia).

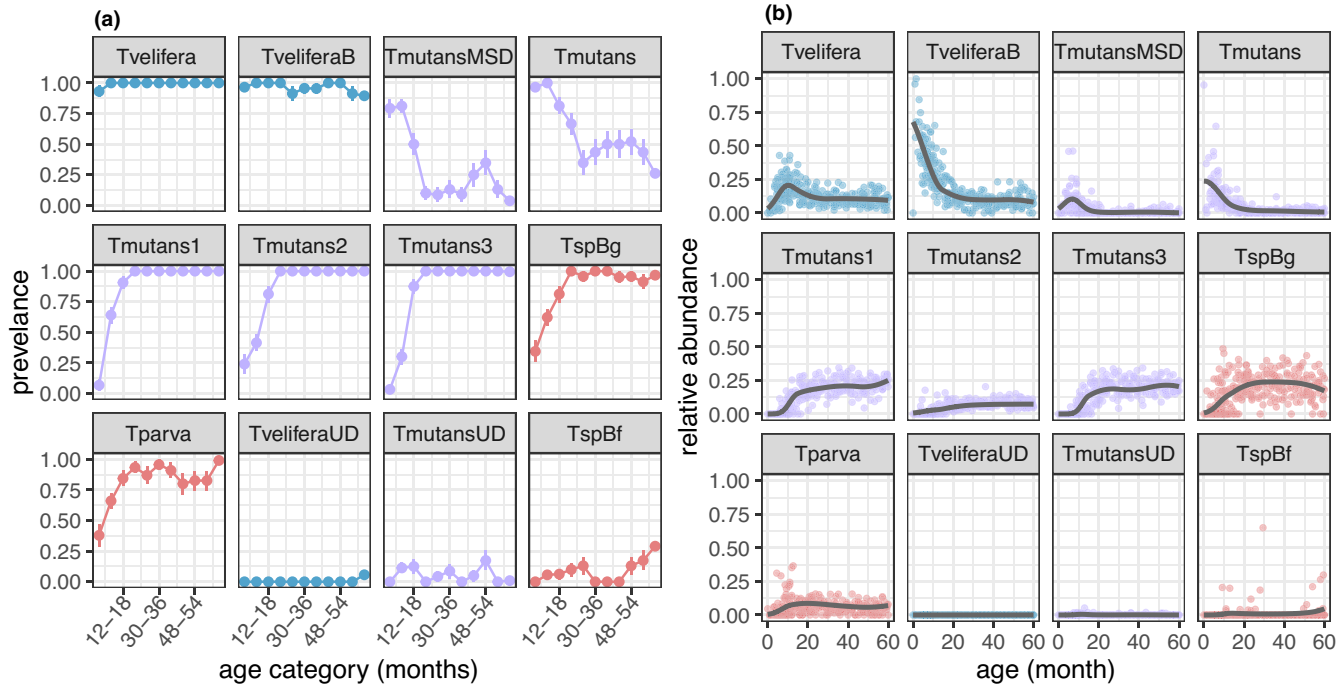

FIGURE 2 Life history variation in *Theileria*. (a) Population-level prevalence curves for each subtype. Points represent prevalence of each subtype within each age bin and vertical lines around each point represent the standard error. (b) Within-host relative abundance by age: The points represent data whereas the lines represent estimates for average relative abundance by age based on model predictions. In (a) and (b), red points include subtypes in the *T. taurotragi* species clade, blue points include subtypes in the *T. velifera* species clade, and purple points include subtypes in the *T. mutans* species clade.

highest average relative abundance in *Theileria* climax communities indicating that these two subtypes are commonly the most abundant within adult animals (Table 1; Figure 2b).

T. sp. (bougasvlei) and *T. parva* exhibited more variable patterns. The average age of first infection was >5 months, however, the 95% confidence interval around this estimate is quite large (Table 1;

TABLE 1 Point estimates for *Theileria* life history infection patterns.

Species clade	Subtype	Age 1st infection	Age at equilibrium	Relative abund at equilibrium
T. velifera	*T. velifera*	0.04 [0.02–0.06]	24.37 [9.92–38.81]	10.29 [7.25–16.24]
	T. velifera B	0.04 [0.02–0.06]	25.25 [9.13–41.36]	0.04 [0–1.25]
	T. velifera UD	NA	NA	NA
T. mutans	*T. mutans*-like 1	6.19 [2.4–9.98]	21 [3.35–38.65]	59.88 [42.4–59.88]
	T. mutans-like 2	1.59 [0–6.45]	15.79 [0.35–31.22]	56.17 [40–59.88]
	T. mutans-like 3	7.8 [3.12–12.47]	22.68 [7.92–37.44]	53.87 [37–59.88]
	T. mutans MSD	0.04 [0–0.09]	17.47 [7.66–27.28]	6.84 [4.79–10.85]
	T. mutans	0.04 [0.02–0.06]	19.38 [8.3–30.46]	0.36 [0–3.25]
	T. mutans UD	NA	NA	NA
T. taurotragi	*T.* sp. (bougasvlei)	0.7 [0–3.15]	25.1 [7.19–43]	34.01 [20.71–59.88]
	T. sp. (buffalo)	11.18 [0–37.26]	0.04 [0–6.84]	59.88 [40.93–59.88]
	T. parva	1.99 [0–5.12]	12.13 [0.78–23.47]	19.61 [9.5–39.42]

Note: Age (months) 1st infection, age (months) at equilibrium, relative abundance at the equilibrium. Estimates include mean [95% confidence interval].

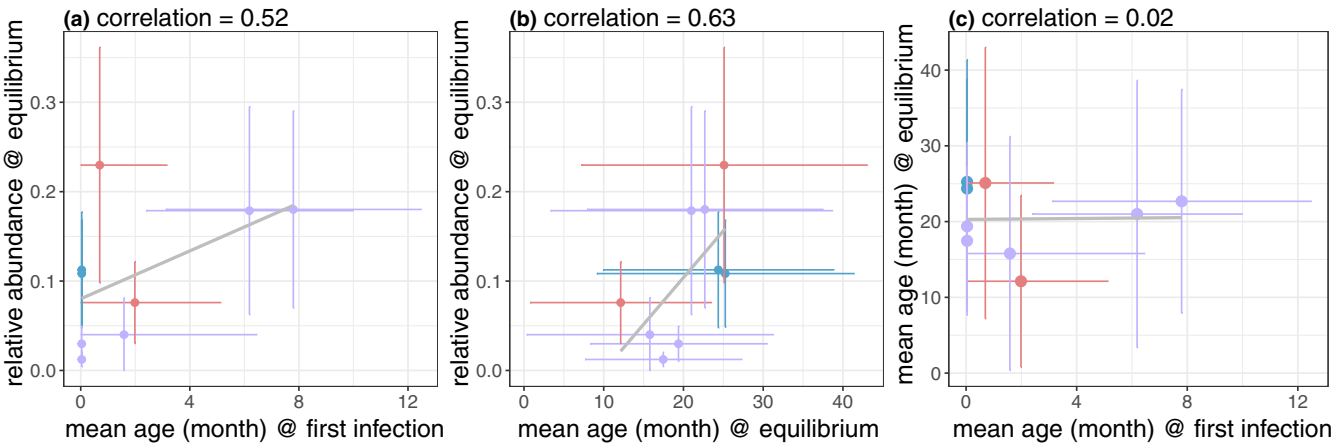

FIGURE 3 Correlations among average life history variables. In each panel (a-c), blue points are subtypes in the *T. velifera* clade, purple points are subtypes in the *T. mutans* clade, and red points are subtypes in the *T. taurotragi* clade. Points represent means and bars represent 95% confidence intervals. Rare subtypes (*T. velifera* undefined, *T. mutans* undefined, and *T.* sp. (buffalo)) are not included.

Figure 2b). Likewise, the mean relative abundance of *T.* sp. (bougasvlei) in climax communities was very variable (95% CI = 0.02–0.35). Prevalence patterns for these subtypes also indicate that some hosts may gain and lose infections throughout their lifetime (Figure 2). Altogether, late colonizing subtypes can also be divided into two life history groups: late-persistent (*T. mutans*-like 1, *T.mutans*-like 2, *T.mutans*-like-3: *T. mutans*-like 1–3) and late-ephemeral (*T. parva*, *T.* sp. (bougasvlei)).

Lastly, *T. velifera* undefined, *T. mutans* undefined and *T.* sp. (buffalo) only infected a small fraction of the host population and did not exhibit clear within-host infection patterns (Figure 2). These subtypes appear to infect buffalo sporadically, perhaps spilling over from other host species that may be more central to their dynamics. As such, these subtypes exhibit no clear life history patterns in buffalo.

When comparing traits, we found a strong positive correlation between mean age at first infection and mean relative abundance at equilibrium (Figure 3a, $\rho = .52$) as well as mean age at equilibrium and relative abundance at equilibrium (Figure 3b, $\rho = .63$). Thus, *Theileria* subtypes that infect hosts early tend not to be as abundant in climax *Theileria* communities as later colonizing subtypes, suggesting a trade-off between dispersal or colonization ability and competitive dominance in this clade of microparasites. This pattern is primarily driven by subtypes in the *T. mutans* clade, as *T. mutans* and *T. mutans* MSD infected all young animals early but were absent in the majority of adult animals (>70%). We found almost no correlation between mean age at first infection and mean age at equilibrium (Figure 3C, $\rho = 0.02$).

Theileria spp. *interaction networks are dynamic and non-linear, with young animals infected by more complex networks than adult animals.*

We used empirical dynamical modelling to quantify interaction networks in juvenile animals (less than or equal to 3 years old) and adult animals (greater than 3 years old) (Figure 4; Table 2; Table S1). We found that interaction networks are non-linear and dynamical, decreasing in complexity with age.

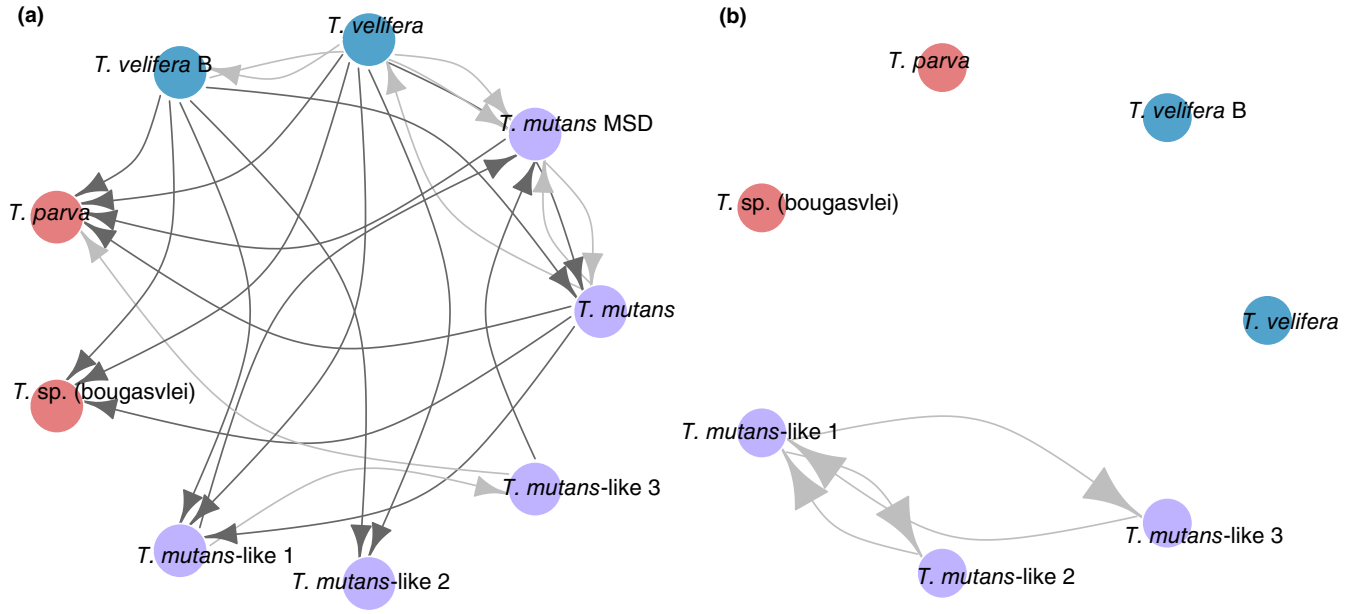

FIGURE 4 *Theileria* interaction network for (a) juvenile and (b) adult animals. Only significant interactions ($p < .05$) are depicted. Arrows indicate the direction of the interaction ($subtype_A \rightarrow subtype_B = species_A$ causes $species_B$). Positive interactions are light grey whereas negative interactions are dark grey. Nodes represent subtypes. Blue nodes are subtypes in the *T. velifera* clade, purple nodes are subtypes in the *T. mutans* clade, and red nodes are subtypes in the *T. taurotragi* clade. The *T. velifera* clade includes early, persistent subtypes; *T. taurotragi* clade are late, ephemeral subtypes; *T. mutans* clade is broken up into early ephemeral (*T. mutans*, *T. mutans* MSD; not in (b) due to low prevalence in adults) and late persistent subtypes (*T. mutans*-like 1–3).

TABLE 2 *Theileria* interaction network summarized by life history strategies.

	EE	LP	EP	LE
Juvenile network				
Early ephemeral (EE)	1.01	−0.07	0.08	−0.61
Late persistent (LP)	−0.96	1.51	0	0.01
Early persistent (EP)	−0.02	−2.38	0.01	−0.34
Late ephemeral (LE)	0	0	0	0
Adult network				
Early ephemeral (EE)	0	0	0	0
Late persistent (LP)	0	1.36	0	0
Early persistent (EP)	0	0	0	0
Late ephemeral (LE)	0	0	0	0

Note: Numbers represent mean significant interaction coefficients. Row causes column. Values were calculated by summing the interaction strength across life history groups. Light grey boxes indicate summed interactions that are positive and dark grey boxes indicate summed interactions that are negative.

Theileria interaction networks differed dramatically between transient successional communities observed in young buffalo and climax *Theileria* communities found in adult hosts. Interactions between *Theileria* subtypes were far more common in juvenile hosts. The *Theileria* interaction network in juvenile buffalo was composed of 23 detectable interactions, including both negative and positive interactions that spanned taxonomic and life history groups. The strongest interactions were generally positive and occurred between *Theileria* subtypes sharing similar life history strategies: early arriving (both persistent and ephemeral) and late-persistent subtypes. A web of negative interactions connected *Theileria* subtypes with contrasting life history patterns and taxonomic affiliations (Table 2; Figure 4). Most notably, on average, the late colonizing subtypes, *T. mutans*-like 1 and *T. mutans*-like 3, had a strong negative effect on the early ephemeral subtype *T. mutans* MSD, while early persistent subtypes in the *T. velifera* clade had a strong negative effect on early ephemeral subtype *T. mutans*.

By contrast, the detectable parasite interaction network in adult animals was composed of only three positive interactions within the *T. mutans* species clade and late-persistent life history group (Table 2; Figure 4). The juvenile and adult network overlapped only

minimally, sharing a single interaction (*T. mutans*-like 1 had a consistent positive effect on *T. mutans*-like 3). In summary, *Theileria* communities in juvenile animals vary in richness and are made up of diverse interaction networks, whereas *Theileria* communities in adult buffalo have ubiquitously high richness with a low number of detectable interactions.

4 | DISCUSSION

Our work provides a picture of the development of microparasite community dynamics over the lifetime of a wild, long-lived mammalian host. In general, we found that microparasite succession patterns reflect those of many free-living communities and follow predictable patterns of succession. Specifically, we found that within-host parasite diversity and among-host community predictability increased with host age: alpha diversity increased while beta-diversity decreased. Underpinning these results, we found that colonization and persistence patterns of individual parasite subtypes were both consistent across individual buffalo and distinct, representing unique life history strategies and deterministic population dynamics. Among life history groups, we observed a negative correlation between the timing of colonization and persistence, reflecting a competition-persistence trade-off. However, unlike free-living communities, we found that the number of detectable interactions decreased with host age and only positive interactions were present in adult communities. We found that the community abundance (% of blood cells infected by *Theileria*) decreased with host age, never exceeding 0.5% of cells infected in animals less than 3 years old, suggesting that *Theileria* may not be resource-limited and thus the change in interaction network and colonization-persistence dynamics may be regulated by host immunity.

In many free-living communities, within-host species richness and evenness (alpha diversity) non-linearly increase following the creation of a habitat patch (Miller & ter Horst, 2012; Patiño et al., 2018; Quesada et al., 2009; Sattler et al., 2010). We found this exact pattern in our buffalo population: buffalo calves were infected with 2–3 *Theileria* subtypes, whereas animals greater than 3 years old were typically infected with 6–10 subtypes, with a small peak in alpha diversity (measured using both the Shannon index and Inverse Simpson) around the three-year mark. The composition of *Theileria* communities became more similar among animals as hosts aged (i.e., declining beta diversity), indicating that the composition of *Theileria* communities in adult animals is largely predictable, similar to climax communities in many free-living systems (Dini-Andreote et al., 2014; Guariguata & Ostertag, 2001; López-Martínez et al., 2013; Martins et al., 2018). We observed a colonization persistence trade-off where some subtypes consistently infected animals less than 2 months old but were cleared by the time animals were greater than 3 years old, while other subtypes only infected older animals but persisted at high relative abundances throughout the lifetime of the animal. This pattern resembles colonization-competition trade-offs observed in numerous ecological systems (e.g., Cadotte et al., 2006; Rodríguez et al., 2007; Smith et al., 2018; Stanton et al., 2002). While our results may stem from niche partitioning that is correlated with temporal changes in the habitat patch (Dini-Andreote et al., 2014), we found that interactions between life history groups displaying the largest colonization-persistence trade-offs (early ephemeral and late persistent subtypes) were negative, supporting a competition-colonization trade-off. Further, early persistent subtypes (*Theileria velifera* clade) negatively affected subtypes across multiple clades and life history groups in young buffalo but were not affected by any subtypes themselves, displaying a uniquely aggressive life history strategy. Finally, in contrast, late ephemeral groups were negatively influenced by both early ephemeral and early persistent groups in young animals and tended to colonize buffalo once relative abundance of these two groups decreased.

Classical succession theory is based upon the concept that habitat patches become increasingly crowded through time, placing restraints on resource availability and ultimately driving interspecific competition (Tilman, 1985). If *Theileria* communities were regulated by host resources (blood cells), we would expect *Theileria* abundance, or % of host cells infected, to increase with host age as a more diverse parasite community composed of increasingly competitive players might exploit the available host resources more efficiently. However, we found that community abundance decreased with host age. The most parsimonious hypothesis is that decreased community abundance is due to the development of more effective acquired immunity and stronger ability to regulate parasite proliferation. The host's adaptive immune responses represent a process fundamentally distinct from the competitive and facilitative interactions that shape free-living communities (Rynkiewicz et al., 2015). Parasite communities' "habitat patches" (i.e. hosts) progressively develop specific resistance against the parasites, effectively reducing parasite reproduction and survival over time. There is not a clear analogy in free-living communities, as top-down regulation by predators does not typically switch through time from distinctly generalized predation to highly specialized, targeted killing. In the *Theileria* system, early successional communities may be regulated by broad, innate immunity of immunologically naïve hoses whereas late successional communities may be regulated by highly subtype-specific adaptive immunity (Doolan et al., 2009; Simon et al., 2015). As such, many of the subtype life histories observed may reflect their unique interactions with the host's immune system through time and the strategy adopted to ensure transmission within the host population. For example, the colonization-persistence trade-off observed in the *T. mutans* clade may be the result of early colonizers invading and quickly replicating within hosts with naive immune systems, whereas persistent subtypes may play a slower strategy based on evasion of specific immune responses in adult hosts.

We found that the change in host interaction network with host age largely supports the idea that *Theileria* life histories and interactions primarily reflect their interactions with the host's immune responses rather than competition for shared resources. Interaction networks in young animals were dense and included positive and negative interactions, whereas interaction networks in adults only

consisted of a few positive interactions within the *T. mutans* clade. This contrasts with free-living communities, where late-stage communities are often characterized by dense negative inter-taxon interactions due to intense competition for limiting resources (e.g., Coyte et al., 2015; Miller & ter Horst, 2012) and/or apparent competition among taxa-sharing generalist consumers. In the *Theileria* parasite community we studied, competitive interactions appear limited to early successional stages, while top-down regulation in climax communities may be mediated by specific immune responses to each subtype—in effect, specialist predators targeting each taxon in the community. Interestingly, increases in adaptive immunity in this parasite community should thus be functionally equivalent to an increase in the density of negative trophic interactions in a free-living system, a process which can promote co-existence of closely related species (Karakoç et al., 2020; Terborgh, 2015; Wallach et al., 2015). Future work quantifying immune effectors (e.g., specific antibodies) against each *Theileria* subtype, and/or manipulating the strength of adaptive immune responses mounted by the host (e.g., by treating with steroids to suppress immune responses (Spaan et al., 2017)), could help to test these ideas.

Our findings have several limitations. Species interactions are notoriously difficult to quantify in observational systems and, while our longitudinal sampling design allowed for advanced causal inference, we may have failed to detect weak interactions due to the length of our sampling interval (Fenton et al., 2014). Additionally, we may have missed some parasite interactions in adult animals as communities were less variable and less suitable for manifold reconstruction than those observed in juvenile animals. While it would be ideal to use experimental approaches to test these ideas, this would be technically and logistically quite challenging in this study system. However, increasing temporal (the number of sampling time points) and spatial (the number of animals) resolution in similar longitudinal observational studies could help with detection of weak interactions, especially in adult hosts (Clark et al., 2015). These limitations notwithstanding, it appears clear that early successional communities in our host–microparasite study consist of much denser interaction networks than late-successional communities. Finally, we represent the network as two snapshots in time. Through empirical dynamical modelling, we calculated an interaction coefficient per buffalo per time step. Next steps include determining how host traits (e.g., immune mediators) influence changes in interaction strength over time.

Overall, individual *Theileria* subtypes follow predictable patterns of succession, leading to changes in community diversity reminiscent of free-living systems. However, unique features of the mammalian immune response may drive disparities in the ecological-evolutionary mechanisms shaping parasite life histories and co-existence.

AUTHOR CONTRIBUTIONS

Caroline K. Glidden, Anna E. Jolles and Brianna Beechler designed the research. Caroline K. Glidden, Anna E. Jolles, Brianna Beechler, Chenyang Duan and Yuan Jiang performed the research. Caroline K. Glidden, Chenyang Duan, Yuan Jiang, Canan Karakoç and Abdul Jabbar contributed new analytical tools. Caroline K. Glidden and Chenyang Duan analysed data. Caroline K. Glidden, Anna E. Jolles, Canan Karakoç, Chenyang Duan and Yuan Jiang wrote the paper. All authors provided feedback and approved the final version of the manuscript.

ACKNOWLEDGEMENTS

This study was supported by the UK Biotechnology and Biological Sciences Research Council grant (BB/L011085/1 awarded to A.E.J.) as part of the joint USDA-NSF- NIH-BBSRC Ecology and Evolution of Infectious Diseases program, the Faculty of Veterinary and Agricultural Sciences, University of Melbourne, under the seed grant scheme Research Initiatives Fund 2018 (awarded to AJ). CKG was supported by an NSF-GRFP, NSF GROW, an ARCS Fellowship, and by an NIH R35 grant (R35GM133439 awarded to Professor Erin A. Mordecai). CD was supported by an NIH R01 grant (R01GM126549 awarded to YJ). We thank the Gasser Lab, particularly Anson Kohler and Robin Gasser, for assistance with the initial molecular work. We thank Adam T. Clark for helpful feedback on the empirical dynamical modelling analysis and the Mordecai Lab for feedback on the final manuscript draft.

CONFLICT OF INTEREST STATEMENT

The authors declare there are no conflicts of interest.

DATA AVAILABILITY STATEMENT

Theileria relative abundance data and meta-data are stored on Dryad: https://doi.org/10.5061/dryad.j6q573nk1. Unique haplotype data are stored in NCBI GenBank GenBank Accession Numbers: MK792966–MK92994.

ORCID

Caroline K. Glidden https://orcid.org/0000-0001-9839-5781
Canan Karakoç https://orcid.org/0000-0002-3921-3535
Yuan Jiang https://orcid.org/0000-0001-6409-9159
Brianna Beechler https://orcid.org/0000-0002-9711-4340
Abdul Jabbar https://orcid.org/0000-0001-8888-0046
Anna E. Jolles https://orcid.org/0000-0003-3074-9912

REFERENCES

Baldwin, C. L., Iams, K. P., Brown, W. C., & Grab, D. J. (1992). Theileria parva: CD4+ helper and cytotoxic T-cell clones react with a schizont-derived antigen associated with the surface of Theileria parva-infected lymphocytes. *Experimental Parasitology*, *75*(1), 19–30. https://doi.org/10.1016/0014-4894(92)90118-t

Budischak, S. A., Hoberg, E. P., Abrams, A., Jolles, A. E., & Ezenwa, V. O. (2016). Experimental insight into the process of parasite community assembly. *Journal of Animal Ecology*, *85*(5), 1222–1233. https://doi.org/10.1111/1365-2656.12548

Budischak, S. A., Wiria, A. E., Hamid, F., Wammes, L. J., Kaisar, M. M. M., van Lieshout, L., Sartono, E., Supali, T., Yazdanbakhsh, M., & Graham, A. L. (2018). Competing for blood: The ecology of parasite resource competition in human malaria-helminth co-infections. *Ecology Letters*, *21*(4), 536–545. https://doi.org/10.1111/ele.12919

Cadotte, M. W., Mai, D. V., Jantz, S., Collins, M. D., Keele, M., & Drake, J. A. (2006). On testing the competition-colonization trade-off in a

multispecies assemblage. *The American Naturalist*, *168*(5), 704–709. https://doi.org/10.1086/508296

Cheng, B., & Tong, H. (1992). On consistent nonparametric order determination and chaos. *Journal of the Royal Statistical Society: Series B (Methodological)*, *54*(2), 427–449. https://doi.org/10.1111/j.2517-6161.1992.tb01890.x

Clark, A. T., Ye, H., Isbell, F., Deyle, E. R., Cowles, J., Tilman, G. D., & Sugihara, G. (2015). Spatial convergent cross mapping to detect causal relationships from short time series. *Ecology*, *96*(5), 1174–1181.

Combrink, L., Glidden, C. K., Beechler, B. R., Charleston, B., Koehler, A. V., Sisson, D., Gasser, R. B., Jabbar, A., & Jolles, A. E. (2020). Age of first infection across a range of parasite taxa in a wild mammalian population. *Biology Letters*, *16*(2), 20190811. https://doi.org/10.1098/rsbl.2019.0811

Connell, J. H. (1978). Diversity in tropical rain forests and coral reefs. *Science*, *199*(4335), 1302–1310.

Couch, C. E., Movius, M. A., Jolles, A. E., Gorman, M. E., Rigas, J. D., & Beechler, B. R. (2017). Serum biochemistry panels in African buffalo: Defining reference intervals and assessing variability across season, age and sex. *PLoS One*, *12*(5), e0176830. https://doi.org/10.1371/journal.pone.0176830

Coyte, K. Z., Schluter, J., & Foster, K. R. (2015). The ecology of the microbiome: Networks, competition, and stability. *Science*, *350*(6261), 663–666. https://doi.org/10.1126/science.aad2602

Csardi, G., & Nepusz, T. (2006). The igraph software package for complex network research. *International Journal of Complex Systems*, 1695 https://igraph.org

Darriba, D., Taboada, G. L., Doallo, R., & Posada, D. (2012). jModelTest 2: More models, new heuristics and parallel computing. *Nature Methods*, *9*(8), 772. https://doi.org/10.1038/nmeth.2109

Devevey, G., Dang, T., Graves, C. J., Murray, S., & Brisson, D. (2015). First arrived takes all: Inhibitory priority effects dominate competition between co-infecting Borrelia burgdorferi strains. *BMC Microbiology*, *15*(1), 61. https://doi.org/10.1186/s12866-015-0381-0

Deyle, E. R., May, R. M., Munch, S. B., & Sugihara, G. (2016). Tracking and forecasting ecosystem interactions in real time. *Proceedings. Biological Sciences*, *283*(1822), 20152258. https://doi.org/10.1098/rspb.2015.2258

Dini-Andreote, F., de Cássia Pereira e Silva, M., Triadó-Margarit, X., Casamayor, E. O., van Elsas, J. D., & Salles, J. F. (2014). Dynamics of bacterial community succession in a salt marsh chronosequence: Evidences for temporal niche partitioning. *The ISME Journal*, *8*(10), 1989–2001. https://doi.org/10.1038/ismej.2014.54

Doolan, D. L., Dobaño, C., & Baird, J. K. (2009). Acquired immunity to malaria. *Clinical Microbiology Reviews*, *22*(1), 13–36. https://doi.org/10.1128/CMR.00025-08

Duan, C., & Jiang, Y. (2022). *Placeholder.* https://ww2.amstat.org/meetings/jsm/2022/onlineprogram/AbstractDetails.cfm?abstractid=323063

Edgar, R. C. (2004). MUSCLE: Multiple sequence alignment with high accuracy and high throughput. *Nucleic Acids Research*, *32*(5), 1792–1797. https://doi.org/10.1093/nar/gkh340

Espínola-Novelo, J. F., González, M. T., Pacheco, A. S., Luque, J. L., & Oliva, M. E. (2020). Testing for deterministic succession in metazoan parasite communities of marine fish. *Ecology Letters*, *23*(4), 631–641. https://doi.org/10.1111/ele.13463

Ezenwa, V. O., & Jolles, A. E. (2015). Epidemiology. Opposite effects of anthelmintic treatment on microbial infection at individual versus population scales. *Science*, *347*(6218), 175–177. https://doi.org/10.1126/science.1261714

Ezenwa, V. O., Jolles, A. E., & O'Brien, M. P. (2009). A reliable body condition scoring technique for estimating condition in African buffalo. *African Journal of Ecology*, *47*(4), 476–481. https://doi.org/10.1111/j.1365-2028.2008.00960.x

Fenton, A., Knowles, S. C. L., Petchey, O. L., & Pedersen, A. B. (2014). The reliability of observational approaches for detecting interspecific parasite interactions: Comparison with experimental results. *International Journal for Parasitology*, *44*(7), 437–445. https://doi.org/10.1016/j.ijpara.2014.03.001

Glidden, C. K., Koehler, A. V., Hall, R. S., Saeed, M. A., Coppo, M., Beechler, B. R., Charleston, B., Gasser, R. B., Jolles, A. E., & Jabbar, A. (2020). Elucidating cryptic dynamics of Theileria communities in African buffalo using a high-throughput sequencing informatics approach. *Ecology and Evolution*, *10*(1), 70–80. https://doi.org/10.1002/ece3.5758

Gloor, G. B., Macklaim, J. M., Pawlowsky-Glahn, V., & Egozcue, J. J. (2017). Microbiome datasets are compositional: And this is not optional. *Frontiers in Microbiology*, *8*, 2224. https://doi.org/10.3389/fmicb.2017.02224

Griffiths, E. C., Pedersen, A. B., Fenton, A., & Petchey, O. L. (2014). Analysis of a summary network of co-infection in humans reveals that parasites interact most via shared resources. *Proceedings of the Royal Society B: Biological Sciences*, *281*(1782), 20132286. https://doi.org/10.1098/rspb.2013.2286

Guariguata, M. R., & Ostertag, R. (2001). Neotropical secondary forest succession: Changes in structural and functional characteristics. *Forest Ecology and Management*, *148*(1), 185–206. https://doi.org/10.1016/S0378-1127(00)00535-1

Gubbels, J. M., de Vos, A. P., van der Weide, M., Viseras, J., Schouls, L. M., de Vries, E., & Jongejan, F. (1999). Simultaneous detection of bovine Theileria and Babesia species by reverse line blot hybridization. *Journal of Clinical Microbiology*, *37*(6), 1782–1789. https://doi.org/10.1128/JCM.37.6.1782-1789.1999

Halliday, F. W., Penczykowski, R. M., Barrès, B., Eck, J. L., Numminen, E., & Laine, A.-L. (2020). Facilitative priority effects drive parasite assembly under coinfection. *Nature Ecology & Evolution*, *4*(11), 1510–1521. https://doi.org/10.1038/s41559-020-01289-9

Hathaway, N. J., Parobek, C. M., Juliano, J. J., & Bailey, J. A. (2018). SeekDeep: Single-base resolution de novo clustering for amplicon deep sequencing. *Nucleic Acids Research*, *46*(4), e21. https://doi.org/10.1093/nar/gkx1201

Hayashida, K., Hara, Y., Abe, T., Yamasaki, C., Toyoda, A., Kosuge, T., Suzuki, Y., Sato, Y., Kawashima, S., Katayama, T., Wakaguri, H., Inoue, N., Homma, K., Tada-Umezaki, M., Yagi, Y., Fujii, Y., Habara, T., Kanehisa, M., Watanabe, H., … Sugimoto, C. (2012). Comparative genome analysis of three eukaryotic parasites with differing abilities to transform leukocytes reveals key mediators of Theileria-induced leukocyte transformation. *MBio*, *3*(5), e00204–e00212. https://doi.org/10.1128/mBio.00204-12

Henrichs, B., Oosthuizen, M. C., Troskie, M., Gorsich, E., Gondhalekar, C., Beechler, B. R., Ezenwa, V. O., & Jolles, A. E. (2016). Within guild co-infections influence parasite community membership: A longitudinal study in African Buffalo. *The Journal of Animal Ecology*, *85*(4), 1025–1034. https://doi.org/10.1111/1365-2656.12535

Hsieh, C., Anderson, C., & Sugihara, G. (2008). Extending nonlinear analysis to short ecological time series. *The American Naturalist*, *171*(1), 71–80. https://doi.org/10.1086/524202

Janeway, C. A., Travers, P., Walport, M., & Shlomchik, M. J. (2001). *Immunobiology* (5th ed.). Garland Science. https://www.ncbi.nlm.nih.gov/books/NBK10757/

Johnson, P. T. J., de Roode, J. C., & Fenton, A. (2015). Why infectious disease research needs community ecology. *Science*, *349*(6252), 1259504. https://doi.org/10.1126/science.1259504

Johnson, P. T. J., & Hoverman, J. T. (2012). Parasite diversity and coinfection determine pathogen infection success and host fitness. *Proceedings of the National Academy of Sciences of the United States of America*, *109*(23), 9006–9011. https://doi.org/10.1073/pnas.1201790109

Jolles, A. E. (2007). Population biology of African buffalo (Syncerus caffer) at Hluhluwe-iMfolozi park, South Africa. *African Journal of Ecology*, *45*, 398–406. https://doi.org/10.1111/j.1365-2028.2006.00726.x

Karakoç, C., & Clark, A. T. (2022). *EDMhelper: A helper package for rEDM. R Package Version 1.0*.

Karakoç, C., Clark, A. T., & Chatzinotas, A. (2020). Diversity and coexistence are influenced by time-dependent species interactions in a predator–prey system. *Ecology Letters*, *23*(6), 983–993. https://doi.org/10.1111/ele.13500

Kröel-Dulay, G., Ransijn, J., Schmidt, I. K., Beier, C., De Angelis, P., de Dato, G., Dukes, J. S., Emmett, B., Estiarte, M., Garadnai, J., Kongstad, J., Kovács-Láng, E., Larsen, K. S., Liberati, D., Ogaya, R., Riis-Nielsen, T., Smith, A. R., Sowerby, A., Tietema, A., & Penuelas, J. (2015). Increased sensitivity to climate change in disturbed ecosystems. *Nature Communications*, *6*(1), 6682. https://doi.org/10.1038/ncomms7682

Kumar, S., Stecher, G., & Tamura, K. (2016). MEGA7: Molecular evolutionary genetics analysis version 7.0 for bigger datasets. *Molecular Biology and Evolution*, *33*(7), 1870–1874. https://doi.org/10.1093/molbev/msw054

Leibold, M. A., & Chase, J. M. (2017). *Metacommunity ecology* (Vol. *59*). Princeton University Press. https://press.princeton.edu/books/hardcover/9780691049168/metacommunity-ecology-volume-59

Lello, J., Boag, B., Fenton, A., Stevenson, I. R., & Hudson, P. J. (2004). Competition and mutualism among the gut helminths of a mammalian host. *Nature*, *428*(6985), 840–844. https://doi.org/10.1038/nature02490

Lewontin, R. C. (1969). The bases of conflict in biological explanation. *Journal of the History of Biology*, *2*(1), 35–45.

López-Martínez, J. o., Hernández-Stefanoni, J. L., Dupuy, J. M., & Meave, J. A. (2013). Partitioning the variation of woody plant β-diversity in a landscape of secondary tropical dry forests across spatial scales. *Journal of Vegetation Science*, *24*(1), 33–45. https://doi.org/10.1111/j.1654-1103.2012.01446.x

Mac Hugh, N. D., Connelley, T., Graham, S. P., Pelle, R., Formisano, P., Taracha, E. L., Ellis, S. A., McKeever, D. J., Burrells, A., & Morrison, W. I. (2009). CD8+ T-cell responses to Theileria parva are preferentially directed to a single dominant antigen: Implications for parasite strain-specific immunity. *European Journal of Immunology*, *39*(9), 2459–2469. https://doi.org/10.1002/eji.200939227

Maddison, W., & Maddison, D. (2008). Mesquite: A modular system for evolutionary analysis. *Evolution*, *62*(5), 1103–1118.

Malkinson, D., Kadmon, R., & Cohen, D. (2003). Pattern analysis in successional communities – An approach for studying shifts in ecological interactions. *Journal of Vegetation Science*, *14*(2), 213–222. https://doi.org/10.1111/j.1654-1103.2003.tb02146.x

Mans, B. J., Pienaar, R., Ratabane, J., Pule, B., & Latif, A. A. (2016). Investigating the diversity of the 18S SSU rRNA hyper-variable region of Theileria in cattle and cape buffalo (Syncerus caffer) from southern Africa using a next generation sequencing approach. *Ticks and Tick-Borne Diseases*, *7*(5), 869–879. https://doi.org/10.1016/j.ttbdis.2016.04.005

Martins, G. M., Arenas, F., Tuya, F., Ramírez, R., Neto, A. I., & Jenkins, S. R. (2018). Successional convergence in experimentally disturbed intertidal communities. *Oecologia*, *186*(2), 507–516. https://doi.org/10.1007/s00442-017-4022-1

McKeever, D. J., Taracha, E. L., Innes, E. L., Mac Hugh, N. D., Awino, E., Goddeeris, B. M., & Morrison, W. I. (1994). Adoptive transfer of immunity to Theileria parva in the CD8+ fraction of responding efferent lymph. *Proceedings of the National Academy of Sciences of the United States of America*, *91*(5), 1959–1963.

Miller, T. E., & ter Horst, C. P. (2012). Testing successional hypotheses of stability, heterogeneity, and diversity in pitcher-plant inquiline communities. *Oecologia*, *170*(1), 243–251. https://doi.org/10.1007/s00442-012-2292-1

Mordecai, E. A., Jaramillo, A. G., Ashford, J. E., Hechinger, R. F., & Lafferty, K. D. (2016). The role of competition—Colonization tradeoffs and spatial heterogeneity in promoting trematode coexistence. *Ecology*, *97*(6), 1484–1496. https://doi.org/10.1890/15-0753.1

Morrison, W. I. (1996). Influence of host and parasite genotypes on immunological control of Theileria parasites. *Parasitology*, *112*(S1), S53–S66. https://doi.org/10.1017/S0031182000076666

Noble, I. R., & Slatyer, R. O. (1977). *Post-fire succession of plants in Mediterranean ecosystems [eucalyptus]. USDA Forest Service General Technical Report WO*. https://scholar.google.com/scholar_lookup?title=Post-fire+succession+of+plants+in+Mediterranean+ecosystems+%5BEucalyptus%5D.&author=Noble+I.R.&publication_year=1977

Norval, R. A. I., Perry, B. D., & Young, A. S. (1992). *The epidemiology of theileriosis in Africa*. ILRI (Aka ILCA and ILRAD).

Oksanen, J. (2020). *vegan: Community Ecology Package*.

Patiño, J., Gómez-Rodríguez, C., Pupo-Correia, A., Sequeira, M., & Vanderpoorten, A. (2018). Trees as habitat islands: Temporal variation in alpha and beta diversity in epiphytic laurel forest bryophyte communities. *Journal of Biogeography*, *45*(8), 1727–1738. https://doi.org/10.1111/jbi.13359

Pickett, S. T. A., Collins, S. L., & Armesto, J. J. (1987). A hierarchical consideration of causes and mechanisms of succession. *Vegetatio*, *69*(1), 109–114. https://doi.org/10.1007/BF00038691

Pienaar, R., Potgieter, F. T., Latif, A. A., Thekisoe, O. M. M., & Mans, B. J. (2011). Mixed Theileria infections in free-ranging buffalo herds: Implications for diagnosing Theileria parva infections in cape buffalo (Syncerus caffer). *Parasitology*, *138*(7), 884–895. https://doi.org/10.1017/S0031182011000503

Poulin, R. (2004). Macroecological patterns of species richness in parasite assemblages. *Basic and Applied Ecology*, *5*(5), 423–434. https://doi.org/10.1016/j.baae.2004.08.003

Quesada, M., Sanchez-Azofeifa, G. A., Alvarez-Añorve, M., Stoner, K. E., Avila-Cabadilla, L., Calvo-Alvarado, J., Castillo, A., Espírito-Santo, M. M., Fagundes, M., Fernandes, G. W., Gamon, J., Lopezaraiza-Mikel, M., Lawrence, D., Morellato, L. P. C., Powers, J. S., de S Neves, F., Rosas-Guerrero, V., Sayago, R., & Sanchez-Montoya, G. (2009). Succession and management of tropical dry forests in the Americas: Review and new perspectives. *Forest Ecology and Management*, *258*(6), 1014–1024. https://doi.org/10.1016/j.foreco.2009.06.023

Raberg, L., de Roode, J. C., Bell, A. S., Stamou, P., Gray, D., & Read, A. F. (2006). The role of immune-mediated apparent competition in genetically diverse malaria infections. *The American Naturalist*, *168*(1), 41–53. https://doi.org/10.1086/505160

Rodríguez, A., Jansson, G., & Andrén, H. (2007). Composition of an avian guild in spatially structured habitats supports a competition–colonization trade-off. *Proceedings of the Royal Society B: Biological Sciences*, *274*(1616), 1403–1411. https://doi.org/10.1098/rspb.2007.0104

Rynkiewicz, E. C., Fenton, A., & Pedersen, A. B. (2019). Linking community assembly and structure across scales in a wild mouse parasite community. *Ecology and Evolution*, *9*(24), 13752–13763. https://doi.org/10.1002/ece3.5785

Rynkiewicz, E. C., Pedersen, A. B., & Fenton, A. (2015). An ecosystem approach to understanding and managing within-host parasite community dynamics. *Trends in Parasitology*, *31*(5), 212–221. https://doi.org/10.1016/j.pt.2015.02.005

Sattler, T., Duelli, P., Obrist, M. K., Arlettaz, R., & Moretti, M. (2010). Response of arthropod species richness and functional groups to urban habitat structure and management. *Landscape Ecology*, *25*(6), 941–954. https://doi.org/10.1007/s10980-010-9473-2

Selik, R. M., Haverkos, H. W., & Curran, J. W. (1984). Acquired immune deficiency syndrome (AIDS) trends in the United States, 1978-1982. *The American Journal of Medicine*, *76*(3), 493–500. https://doi.org/10.1016/0002-9343(84)90669-7

Simon, A. K., Hollander, G. A., & McMichael, A. (2015). Evolution of the immune system in humans from infancy to old age. *Proceedings of the Royal Society B: Biological Sciences*, *282*(1821), 20143085. https://doi.org/10.1098/rspb.2014.3085

Simpson, G. (2022). *Gratia: Graceful ggplot-based graphics and other functions for GAMs fitted using mgcv. R Package Version 0.7.3*. https://gavinsimpson.github.io/gratia/

Smith, G. R., Steidinger, B. S., Bruns, T. D., & Peay, K. G. (2018). Competition–colonization tradeoffs structure fungal diversity. *The ISME Journal*, *12*(7), 1767. https://doi.org/10.1038/s41396-018-0086-0

Spaan, J. M., Pitts, N., Buss, P., Beechler, B., Ezenwa, V. O., & Jolles, A. E. (2017). Noninvasive measures of stress response in African buffalo (Syncerus caffer) reveal an age-dependent stress response to immobilization. *Journal of Mammalogy*, *98*(5), 1288–1300. https://doi.org/10.1093/jmammal/gyx073

Stanton, M. L., Palmer, T. M., & Young, T. P. (2002). Competition–colonization trade-offs in a guild of African Acacia-ants. *Ecological Monographs*, *72*(3), 347–363. https://doi.org/10.1890/0012-9615(2002)072[0347:CCTOIA]2.0.CO;2

Sugihara, G., May, R., Ye, H., Hsieh, C., Deyle, E., Fogarty, M., & Munch, S. (2012). Detecting causality in complex ecosystems. *Science*, *338*(6106), 496–500. https://doi.org/10.1126/science.1227079

Sugihara, G., & May, R. M. (1990). Nonlinear forecasting as a way of distinguishing chaos from measurement error in time series. *Nature*, *344*(6268), 734–741. https://doi.org/10.1038/344734a0

Takens, F. (1981). Detecting strange attractors in turbulence. In D. Rand & L.-S. Young (Eds.), *Dynamical systems and turbulence*, *Warwick 1980* (pp. 366–381). Springer. https://doi.org/10.1007/BFb0091924

Telfer, S., Lambin, X., Birtles, R., Beldomenico, P., Burthe, S., Paterson, S., & Begon, M. (2010). Species interactions in a parasite community drive infection risk in a wildlife population. *Science*, *330*(6001), 243–246. https://doi.org/10.1126/science.1190333

Terborgh, J. W. (2015). Toward a trophic theory of species diversity. *Proceedings of the National Academy of Sciences of the United States of America*, *112*(37), 11415–11422. https://doi.org/10.1073/pnas.1501070112

Tilman, D. (1985). The resource-ratio hypothesis of plant succession. *The American Naturalist*, *125*(6), 827–852.

Tilman, D. (1994). Competition and biodiversity in spatially structured habitats. *Ecology*, *75*(1), 2–16. https://doi.org/10.2307/1939377

Wallach, A. D., Ripple, W. J., & Carroll, S. P. (2015). Novel trophic cascades: Apex predators enable coexistence. *Trends in Ecology & Evolution*, *30*(3), 146–153. https://doi.org/10.1016/j.tree.2015.01.003

Wood, S. (2017). *Generalized additive models: An introduction with R* (2nd ed.). Chapman and Hall/CRC.

Ye, H., Deyle, E. R., Gilarranz, L. J., & Sugihara, G. (2015). Distinguishing time-delayed causal interactions using convergent cross mapping. *Scientific Reports*, *5*(1), 14750. https://doi.org/10.1038/srep14750

Zeilis, A., & Grothendieck, G. (2019). Zoo: S3 infrastructure for regular and irregular time series. *Journal of Statistical Software*, *14*(6), 1–27. https://doi.org/10.18637/jss.v014.i06

SUPPORTING INFORMATION

Additional supporting information can be found online in the Supporting Information section at the end of this article.

How to cite this article: Glidden, C. K., Karakoç, C., Duan, C., Jiang, Y., Beechler, B., Jabbar, A., & Jolles, A. E. (2023). Distinct life history strategies underpin clear patterns of succession in microparasite communities infecting a wild mammalian host. *Molecular Ecology*, *00*, 1–14. https://doi.org/10.1111/mec.16949